Journal of Sound and Vibration (1994) **169**(2), 179–196

TRANSVERSE VIBRATION OF AN AXIALLY ACCELERATING STRING

M. PAKDEMIRLI

Department of Engineering Science and Mechanics, Virginia Polytechnic Institute and State University, Blacksburg, Virginia 24061, *U.S.A.*

A. G. ULSOY

Department of Mechanical Engineering and Applied Mechanics, The University of Michigan, Ann Arbor, Michigan 48109-2125, *U.S.A.*

AND

A. CERANOGLU

Department of Mechanical Engineering, Bogazici University, Turkey

(*Received* 2 *March* 1992, *and in final form* 13 *July* 1992)

The transverse vibration of an axially accelerating string is investigated. The equation of motion is developed using Hamilton's principle. The resulting partial differential equations are discretized using Galerkin's method. Assuming the axial velocity to be periodic, a stability analysis is performed using Floquet theory. One-, two-, three-, four-, six- and eight-term series approximations are considered in the Galerkin's method. The one-term approximation leads to a Mathieu equation, the solution of which is well known. The numerical results for one term are compared with the analytical solution for the Mathieu equation, and they are in full agreement. The two-term approximation leads to gyroscopically coupled equations, and the solutions differ significantly from that of the one-term approximation, whereas the three-term approximation solutions look similar to the one-term approximation solutions. The analysis is carried out for higher order even approximations and the solutions are in qualitative agreement. The two- and four-term approximation solutions are compared with the analytical results from Hsu's method, and are in reasonable agreement. The results show that instabilities occur at much higher amplitudes and frequencies of the periodic axial velocity than that of typical devices such as tape machines and band saws.

1. INTRODUCTION

Many technological devices involve the transverse vibration of axially moving materials. High speed fiber winding, magnetic tape systems, thread lines, band saw blades, belts and pipes transporting fluids all belong to this class. Numerous researchers have examined the dynamic response of such systems. The early research in this area includes studies by Skutch [1] and Sack [2]. The work done up to 1978 has been reviewed by Ulsoy, Mote and Szymani [3], and a more recent review is given by Wickert and Mote [4]. Basic characteristics of such devices include a transport velocity dependent natural frequency spectrum, and the existence of a critical speed at which a divergence instability occurs [3]. Among the studies reviewed in reference [3] are several investigations of parametric instability due to axial tension variations and periodic edge loads in strings and bands moving axially at constant velocity. More recently, Ulsoy and Mote [5] have used an axially

0022-460X/94/020179 + 18 $08.00/0

moving plate model to investigate the role of in-plane stresses in the transverse vibration of band saw blades. The coupled vibrations of the belt and tensioner in automotive accessory drive systems has also been experimentally and analytically investigated [6]. Chonan [7] studied the steady state response of the axially moving thick beam subjected to a concentrated constant lateral force. Recently, Wickert and Mote [8] showed that the total mechanical energy associated with an axially moving string or beam that travels between two supports is not constant, but varies at twice the frequency of free oscillations. The same authors [9] examined an axiallly moving monocable ropeway with attached masses. They also presented a modal analysis for the axially moving string and the travelling beam [10].

In all these works, the axial transport velocity was taken to be constant. However, many systems are subject to accelerations and decelerations, which in fact may seriously change the vibration behaviour. The equation of motion for the transverse vibration of an axially accelerating string was derived by Miranker [11], but no solution was presented. In the present study, the case in which velocity is not constant but a prescribed function of time is treated. The partial differential equation governing the motion are derived. Discretization of the partial differential equation by Galerkin's method gives a system of n ordinary differential equations. In the present analysis, up to eight-term approximations based upon the eigenfunctions of the stationary string are considered (i.e., $n = 1, 2, 3, 4, 6, 8$). The time dependent axial velocity function $v(t)$ is assumed to be sinusoidal. A stability analysis for each approximation is carried out using Floquet theory. Taking only one term in Galerkin's approximation results in the standard Mathieu equation, the solution of which is well known. Taking two terms, the resulting two ordinary differential equations are gyroscopically coupled and periodic. The two-term approximation and one-term approximation solutions differ greatly, whereas three-term approximation solutions are similar to those of the one-term approximation. The even-term approximations capture the gyroscopic coupling and represent the physics of the system more accurately. Thus, the four-, six- and eight-term approximations are considered. While a qualitative agreement is evident among the even-term approximations, increasing the number of terms in the approximation improves the quantitative results. Finally, the two-term and four-term Floquet solutions are compared to the analytical solution presented in reference [12] and show reasonable agreement. The results show that instabilities occur for sinusoidal transport velocities when the amplitude and frequency of the velocity become large.

2. EQUATIONS OF MOTION

The physical model considered, and shown in Figure 1, is a continuous string or strip passing over two pulleys at a transport velocity $v(t)$. The velocity is not constant, but is assumed to be a prescribed function of time.

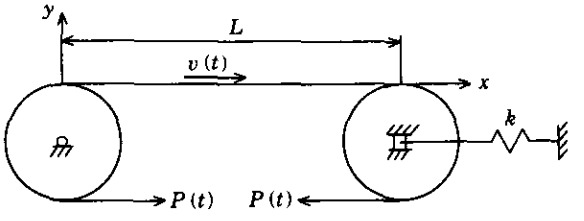

Figure 1. Co-ordinates and geometry.

According to Hamilton's principle [13],

$$\delta \int_{t_1}^{t_2} (T - V)\,\mathrm{d}t = 0, \tag{1}$$

where δ denotes the variation. The kinetic energy T is

$$T = \frac{\rho A}{2} \int_0^L [(\dot{y} + vy')^2 + v^2]\,\mathrm{d}x, \tag{2}$$

where ρ is the density, A is the cross-sectional area, L is the length, y is the transverse displacement and v is the axial velocity of the string. Note that $(\cdot)$ denotes the derivative with respect to time and $(\,)'$ denotes the derivative with respect to the spatial variable x. The potential energy V is

$$V = \int_0^L \left[Pe + \frac{EA}{2} e^2 + F\Delta \right] \mathrm{d}x, \tag{3}$$

where P is the tension in the string, e represents the strain, E is Young's modulus, F is an arbitrary driving force and Δ is the total longitudinal displacement of the system. The first term in the integral in equation (3) is due to the tension force P, the second term is due to axial deformation and the third term is the work done by the arbitrary driving force F. It is assumed that the tension force P is large and that the flexural rigidity of the string or strip is negligibly small.

The strain can be written as [14]

$$e = (1 + (y')^2)^{1/2} - 1, \tag{4}$$

and inserting equation (4) into equation (3), then equations (3) and (2) into equation (1), one obtains

$$\delta \int_{t_1}^{t_2} \int_0^L \left\{ \frac{\rho A}{2} [\dot{y}^2 + 2\dot{y}vy' + v^2(y')^2 + v^2] - P[(1 + (y')^2)^{1/2} - 1] \right.$$

$$\left. - \frac{EA}{2} [1 + (y')^2 + 1 - 2(1 + (y')^2)^{1/2}] - F\Delta \right\} \mathrm{d}x\,\mathrm{d}t = 0. \tag{5}$$

Taking the variation with respect to v, Δ and y, rearranging the terms and writing $\delta\dot{\Delta}$ instead of δv, the expression in equation (5) becomes

$$\int_{t_1}^{t_2} \int_0^L \left\{ \rho A[\dot{y}y' + v(y')^2 + v]\delta\dot{\Delta} - F\delta\Delta + \rho A[(\dot{y} + vy')\delta\dot{y} + (\dot{y}v + v^2y')\delta y'] \right.$$

$$\left. - [Py'/(1 + (y')^2)^{1/2} - EAy'(1 - 1/(1 + (y')^2)^{1/2})]\delta y' \right\} \mathrm{d}x\,\mathrm{d}t = 0. \tag{6}$$

Now applying integration by parts to the first two terms in the integral in equation (6), equating to zero, and eliminating the higher order terms, one obtains the equation

$$F = \rho A\dot{v}. \tag{7}$$

The driving force $F(t)$ is arbitrary, so $v(t)$ is also arbitrary, and equation (7) does not restrict the choice of the transport velocity.

Taking the remaining terms in the integral in equation (6), applying integration by parts, equating to zero, and eliminating the higher order terms, the equation of transverse

vibration is obtained as

$$\rho A(\ddot{y} + \dot{v}y' + 2v\dot{y}') + (\rho Av^2 - P)y'' = 0. \tag{8}$$

This linear equation of motion for the transverse vibration of the axially moving string is valid for small displacements y, and for large values of P, the tension force. Equation (8) has also been presented in reference [11]. However, its solution has not been studied, and that will be the goal of the following analysis.

3. SOLUTION METHODS

Galerkin's method [14] is applied to solve equation (8). The trial function is chosen to be of the form,

$$y(x, t) = \sum_{i=1}^{n} q_i(t) \sin(i\pi x/L), \tag{9}$$

where $\sin(i\pi x/L)$ is the ith eigenfunction of the simply supported stationary string, and the $q_i(t)$ are generalized displacements. Taking the appropriate derivatives and substituting into equation (8), one obtains the residual

$$R = \sum_{i=1}^{n} \left\{ \rho A\ddot{q}_i \sin\frac{i\pi x}{L} + 2\rho Av\frac{i\pi}{L}\dot{q}_i \cos\frac{i\pi x}{L} + \rho A\dot{v}\frac{i\pi}{L}q_i \cos\frac{i\pi x}{L} + (P - \rho Av^2)\left(\frac{i\pi}{L}\right)^2 q_i \sin\frac{i\pi x}{L} \right\}. \tag{10}$$

Application of Galerkin's method requires that

$$\int_0^L R w_j(x)\,dx = 0, \qquad j = 1, 2, \ldots, n. \tag{11}$$

The weighting functions $w_j(x)$ are also the stationary string eigenfunctions [15]

$$w_j(x) = \sin(j\pi x/L). \tag{12}$$

Inserting equations (10) and (12) into equation (11) and integrating yields a set of ordinary differential equations of the form

$$\mathbf{M}\ddot{\mathbf{q}} + \mathbf{C}\dot{\mathbf{q}} + \mathbf{K}\mathbf{q} = \mathbf{0}, \tag{13}$$

where the elements of the matrices in equation (13) are defined as

$$m_{ji} = \int_0^L \left(\sin\frac{i\pi x}{L}\sin\frac{j\pi x}{L}\right)dx = \begin{cases} L/2, & \text{if } i = j, \\ 0, & \text{if } i \neq j, \end{cases} \tag{14}$$

$$c_{ji} = \int_0^L \left(\frac{2\pi iv}{L}\cos\frac{i\pi x}{L}\sin\frac{j\pi x}{L}\right)dx = \begin{cases} 0 & , \quad \text{if } i = j, \\ 0 & , \quad \text{if } i \neq j,\ i + j = 2n, \\ 4ijv/(j^2 - i^2), & \text{if } i \neq j,\ i + j = 2n + 1, \end{cases} \tag{15}$$

$$k_{ji} = \int_0^L \left\{\left(\frac{P}{\rho A} - v^2\right)\left(\frac{i\pi}{L}\right)^2 \sin\frac{i\pi x}{L}\sin\frac{j\pi x}{L} + \frac{\dot{v}\pi i}{L}\cos\frac{i\pi x}{L}\sin\frac{j\pi x}{L}\right\}dx$$

$$= \begin{cases} (P/(\rho A) - v^2)(i\pi/L)^2 L/2, & \text{if } i = j, \\ 0 & , \quad \text{if } i \neq j,\ i + j = 2n, \\ 2\dot{v}ij/(j^2 - i^2) & , \quad \text{if } i \neq j,\ i + j = 2n + 1. \end{cases} \tag{16}$$

Taking the first term in the series solution (9), equation (13) reduces to a scalar ordinary differential equation:

$$\ddot{q}_1 + \left(\frac{P}{\rho A} - v^2\right)\frac{\pi^2}{L^2} q_1 = 0. \tag{17}$$

Taking two terms in the series solution (9), equation (13) reduces to a set of coupled ordinary differential equations

$$\begin{bmatrix} 1 & 0 \\ 0 & 1 \end{bmatrix}\begin{bmatrix} \ddot{q}_1 \\ \ddot{q}_2 \end{bmatrix} + \begin{bmatrix} 0 & -\dfrac{16v}{3L} \\ \dfrac{16v}{3L} & 0 \end{bmatrix}\begin{bmatrix} \dot{q}_1 \\ \dot{q}_2 \end{bmatrix} + \begin{bmatrix} \left(\dfrac{P}{\rho A} - v^2\right)\dfrac{\pi^2}{L^2} & -\dfrac{8\dot{v}}{3L} \\ \dfrac{8\dot{v}}{3L} & \left(\dfrac{P}{\rho A} - v^2\right)\dfrac{4\pi^2}{L^2} \end{bmatrix}\begin{bmatrix} q_1 \\ q_2 \end{bmatrix} = 0. \tag{18}$$

Higher order approximate equations can also be written by evaluating equations (14)–(16) in a similar manner. These approximate solutions employ admissible functions and will converge to the exact solution as the number of terms is increased. Equation (18) introduces features of the problem which are not evident in the one-term approximation in equation (17); namely, the skew symmetric gyroscopic matrix multiplying the generalized velocities, and the skew symmetric coupling terms in the stiffness matrix. The gyroscopic coupling terms are known to be significant in the constant axial velocity case [3]. Note also that both the gyroscopic and stiffness matrices contain time varying parameters due to the presence of the velocity $v(t)$ and acceleration $\dot{v}(t)$. Higher order, even-term approximations share common properties with that of the two-term approximation in equation (18).

4. RESULTS AND DISCUSSION

The solutions of equations (17) and (18) corresponding to one- and two-term approximations, respectively, as well as the higher order approximations, will be presented here for a particular velocity function $v(t)$. Consider the system to have a variation of velocity that increases from start-up, reaching a maximum and then decreasing to zero. This is the ideal case in which acceleration is constant and followed by an equal constant deceleration phase. However, taking the velocity as a sine function and the acceleration as a cosine function will be more realistic, since abrupt changes in velocity and acceleration are not typically observed in physical systems. Therefore, the axial velocity will be written here as

$$v(t) = v_0 \sin \omega_0 t, \tag{19}$$

where v_0 is the axial velocity amplitude and ω_0 is the frequency of axial velocity variation.

The tension force in the band or string varies with velocity according to the following relation [16]:

$$P = P_0 + \eta \rho A v^2, \tag{20}$$

where P_0 is the initial tension and $0 \leqslant \eta \leqslant 1$. One can also define a pulley support parameter $\kappa = 1 - \eta$, the value of which depends on the pulley support system. In constant displacement mechanisms, such as tapes, κ can be taken as 1 (i.e., in Figure 1, $k = \infty$). In constant tension mechanisms, $\kappa = 0$ (i.e., in Figure 1, $k = 0$). See reference [16] for a derivation of the pulley support parameters.

4.1. ONE-TERM APPROXIMATION

Inserting equation (19) and (20) into equation (17) and using $\kappa = 1 - \eta$ leads to

$$\ddot{q}_1 + \left(\frac{P_0}{\rho A} - \kappa v_0^2 \sin^2 \omega_0 t\right)\frac{\pi^2}{L^2} q_1 = 0. \tag{21}$$

Using the trigonometric identity

$$\sin^2 \omega_0 t = (1 - \cos 2\omega_0 t)/2 \tag{22}$$

and defining $t' = w_0 t$ yields

$$\frac{d^2 q_1}{dt'^2} + \left\{\left(\frac{2P_0}{\rho A} - \kappa v_0^2\right)\frac{\pi^2}{2\omega_0^2 L^2} + \left(\frac{2\kappa v_0^2 \pi^2}{4w_0^2 L^2}\right)\cos 2t'\right\} q_1 = 0. \tag{23}$$

Comparing equation (23) to the standard Mathieu equation [17]

$$\frac{d^2 q_1}{dt'^2} + (\delta + 2\varepsilon \cos 2t')q_1 = 0, \tag{24}$$

one can define

$$\delta = \left(\frac{2P_0}{\rho A} - \kappa v_0^2\right)\frac{\pi^2}{2\omega_0^2 L^2}, \qquad \varepsilon = \frac{\kappa v_0^2 \pi^2}{4w_0^2 L^2}. \tag{25}$$

The well known solution of the Mathieu equation (e.g., reference [17]) is presented for convenience here in the form of a Strutt diagram in Figure 2. The solution leads to stability

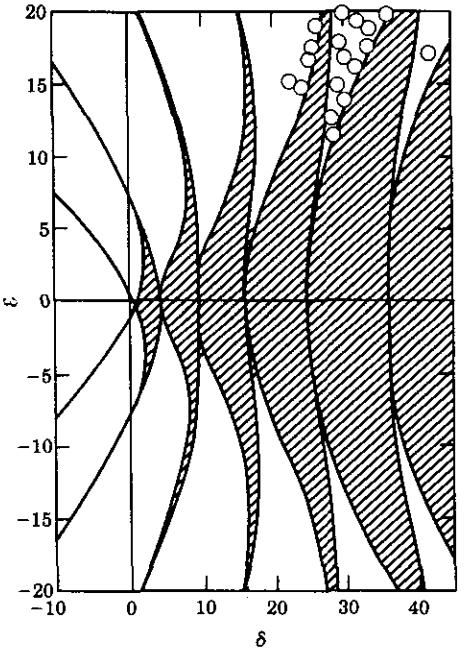

Figure 2. Mathieu stability (shaded) and instability areas (from reference [17]). Floquet results for unstable points are indicated on the graphs as points.

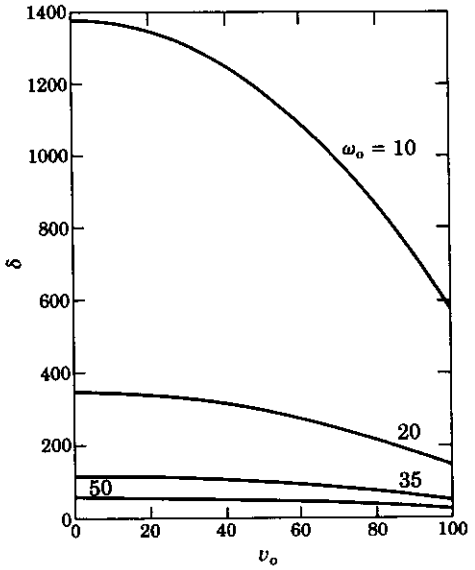

Figure 3. δ *vs.* v_0 for specific ω_0 values (indicated on the curves).

and instability regions, where the shaded areas in Figure 2 represent the stable regions. The aim, therefore, in design is to ensure operation in the stable region.

A computer code, valid for any n-term approximation, was developed to integrate the equations over one period by an adaptive step size Runge–Kutta subroutine, calculate the monodromy matrix and then obtain the eigenvalues or Floquet multipliers of the system [18]. Numerical calculations are performed in the interval $0 < v_0 \leqslant 100$ and $0 < \omega_0 \leqslant 50$, and yield the unstable points indicated by the open circles on Figure 2. Although most of the points lie outside the region shown in the plot, the ones inside

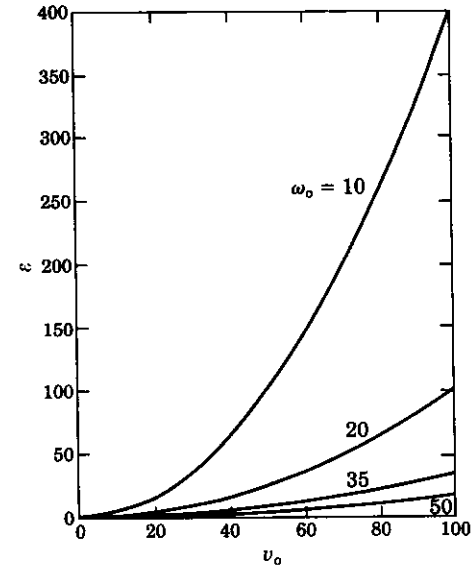

Figure 4. ε *vs.* v_0 for specific ω_0 values (indicated on the curves).

TABLE 1

Standard parameter values used

Parameter	Standard value	Unit
P_0	76·22	N
ρ	7754·0	kg/m^3
A	$0{\cdot}5202 \times 10^{-5}$	m^2
κ	0·22	
L	0·3681	m

show full agreement with the analytical results. This is the case because a small area in the v_0–ω_0 plane is mapped to a very large area in the δ–ε plane, thereby making the solutions highly sensitive to the given v_0 and w_0 values. The relations between δ, ε and v_0, ω_0 can be more easily seen in Figures 3 and 4. In all numerical calculations, the parameters for a table top band saw, as given in reference [5] and summarized in Table 1, were used.

Examining the definitions of δ and ε from equation (25), one sees that P_0 and v_0 are important parameters influencing δ and ε. The parameter v_0 appears in the expressions for both δ and ε; increasing v_0 increases ε and decreases δ. Thus, one concludes that the possibility of instability is greater at high speeds. P_0 influences δ only, and increasing P_0 increases δ without any change in ε. Thus, increasing P_0 may be useful for stability. The constant κ is another parameter which alters the magnitude of δ and ε and, as discussed previously, depends on the pulley support configuration.

4.2. HIGHER ORDER APPROXIMATIONS

For higher order approximations, solutions are obtained using the same computer code described previously. The program calculates the monodromy matrix and finds the magnitudes of the eigenvalues of the matrix. If all the magnitudes of eigenvalues are less than 1, the solutions are stable; if all are equal to 1, the solutions are periodic and bounded; and if at least one of them is greater than 1, the system is unstable [18]. For even approximations, if λ is an eigenvalue then $1/\lambda$ is also an eigenvalue. Therefore, bounded or stable solutions are obtained only if all the magnitudes of eigenvalues are equal to 1, in agreement with reference [19]. As in the case of a one-term approximation, this is not true for the three-term approximation. The one- and three-term approximation solutions look qualitatively similar, whereas the even-term approximations differ significantly from the odd-term approximations. For a detailed discussion of parametric stability, the reader is referred to references [20, 21].

The program was also checked for the two- and four-term approximations against the known constant velocity solutions given in reference [22], and is in full agreement.

Even approximations are expected to be better in modelling the physical system, since they lead to gyroscopically coupled terms; preliminary calculations were first performed for $n = 2, 4, 6$ and 8. The results are displayed in the v_0–ω_0 plane for 1250 points in the intervals $0 < v_0 \leqslant 100$, $0 < \omega_0 \leqslant 100$ and $10 \leqslant \omega_0 \leqslant 50$ with an increment of 2 for each parameter. The results show that all approximations agree that the critical instability region is at $v_0 \geqslant 70$, $\omega_0 \geqslant 10$. Since 100 for v_0 and 50 for ω_0 were considered as the maximum values, the region of interest becomes $70 \leqslant v_0 \leqslant 50$. For this region a step size of 1 is chosen, and the calculations are repeated for all even approximations

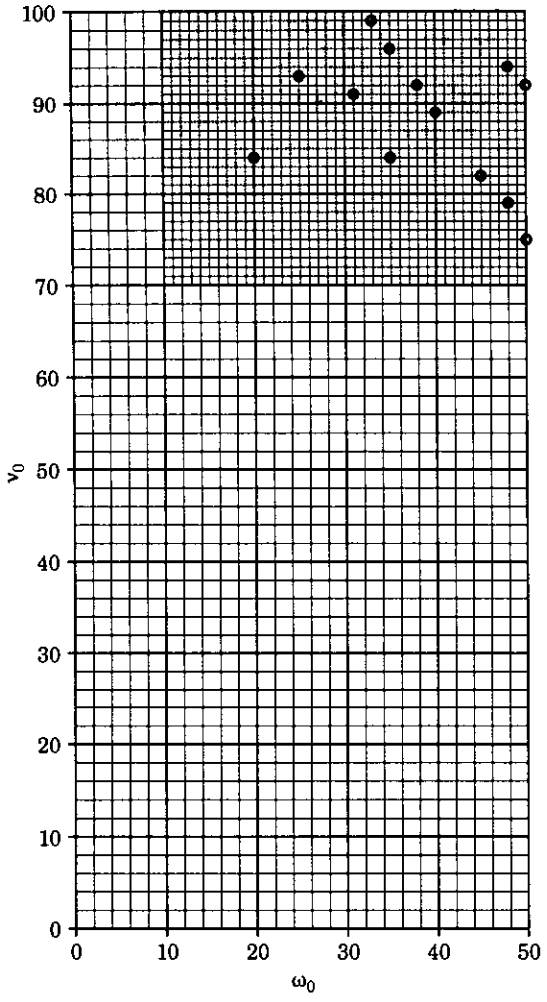

Figure 5. Two-term approximation stable and unstable points in the v_0–ω_0 plane (all intersection points without a label indicate stable points, whereas circled ones indicate unstable points).

for 1271 points. The combined results are shown in Figures 5–8. In these figures, all intersection points are stable except the points marked with an open circle, which are unstable. The finer grid region is shown within the coarse grid for convenience. Although agreement between the $n = 2, 4, 6$ and 8 approximations in the coarse grid region is evident, this is not the case for the finer grid region. As the number of terms in the approximation is increased, one obtains more unstable points and at lower frequencies. This trend is in agreement with the analytical solution presented in the next section. As one increases the number of terms, the unstable points tend to cluster, and represent a better defined instability region. However, there are some disjointed points even in the eight-term approximation. This happens because the equations are highly sensitive to the v_0 and ω_0 values and, as a consequence, a small area in the v_0–ω_0 plane is mapped into a very large area in the δ–ε plane. To better identify the instability boundaries, a very fine grid of step size 0·2 is taken for both parameters in the intervals $90 \leqslant v_0 \leqslant 95$ and $45 \leqslant \omega_0 \leqslant 50$ for the eight-term approximation. The result is shown in

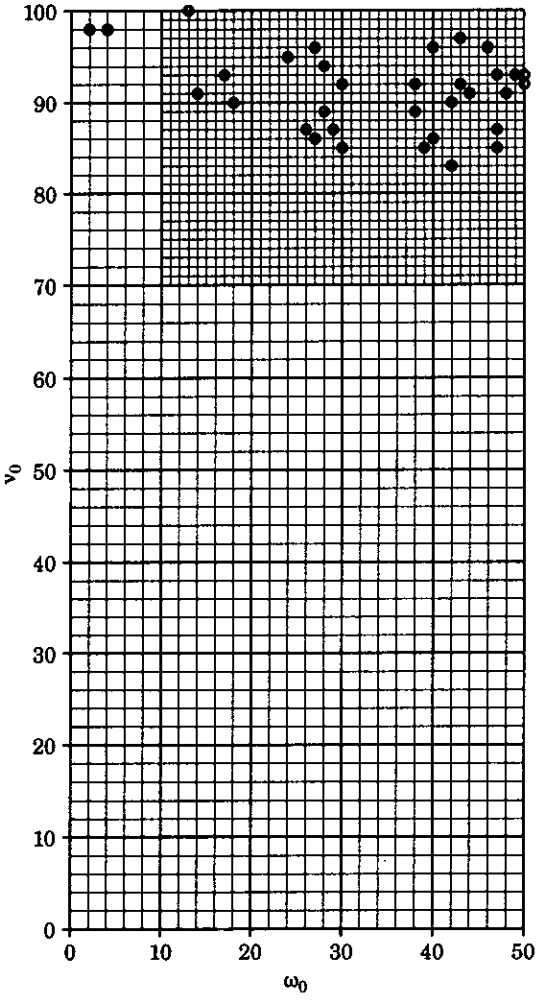

Figure 6. Four-term approximation stable and unstable points in the v_0–ω_0 plane (all intersection points without a label indicate stable points, whereas circled ones indicate unstable points).

Figure 9, where it is evident that the equations are highly sensitive to the v_0 and ω_0 parameters.

For some unstable points, the Floquet solutions were checked using time integration results and they are in full agreement. Two simulation results, for two- and four-term approximations, are presented in Figures 10 and 11, respectively, for the first generalized displacement $q_1(t)$. It can easily be seen that the instability is strong in the lower-term approximations, whereas it tends to be weaker for the higher order approximations. Finally, the calculated Floquet multipliers for the two-term and four-term approximations are given in Tables 2 and 3, respectively. Only the unstable points are given.

4.3. COMPARISON WITH ANALYTICAL RESULTS

To compare the results in the previous section with the analytical solution given in reference [12], first insert equations (19) and (20) into equation (18) and then use the

identity (22) to obtain

$$\begin{bmatrix} 1 & 0 \\ 0 & 1 \end{bmatrix}\begin{bmatrix} \ddot{q}_1 \\ \ddot{q}_2 \end{bmatrix} + \begin{bmatrix} 0 & -\dfrac{16v_0}{3L}\sin\omega_0 t \\ \dfrac{16v_0}{3L}\sin\omega_0 t & 0 \end{bmatrix}\begin{bmatrix} \dot{q}_1 \\ \dot{q}_2 \end{bmatrix}$$
$$+ \begin{bmatrix} \left(\dfrac{2P_0}{\rho A} - \kappa v_0^2 + \kappa v_0^2 \cos 2\omega_0 t\right)\dfrac{\pi^2}{2L^2} & -\dfrac{8v_0\omega_0}{3L}\cos\omega_0 t \\ \dfrac{8v_0\omega_0}{3L}\cos\omega_0 t & \left(\dfrac{2P_0}{\rho A} - \kappa v_0^2 + \kappa v_0^2 \cos 2\omega_0 t\right)\dfrac{2\pi^2}{L^2} \end{bmatrix}\begin{bmatrix} q_1 \\ q_2 \end{bmatrix} = \mathbf{0}. \tag{26}$$

For equation (26), a general analytical solution is not available. However, a perturbation solution is available for ϵ small in the equations [12]

$$\ddot{\mathbf{X}} + \epsilon \mathbf{C}(t)\dot{\mathbf{X}} + (\mathbf{B}(0) + \epsilon \mathbf{B}(t))\mathbf{X} = \mathbf{0}. \tag{27}$$

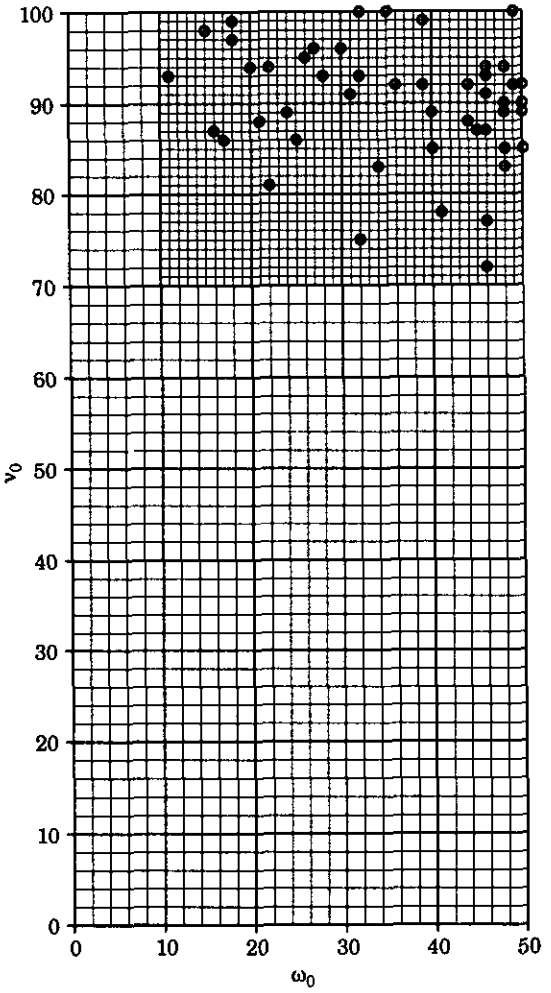

Figure 7. Six-term approximation stable and unstable points in the v_0–ω_0 plane (all intersection points without a label indicate stable points, whereas circled ones indicate unstable points).

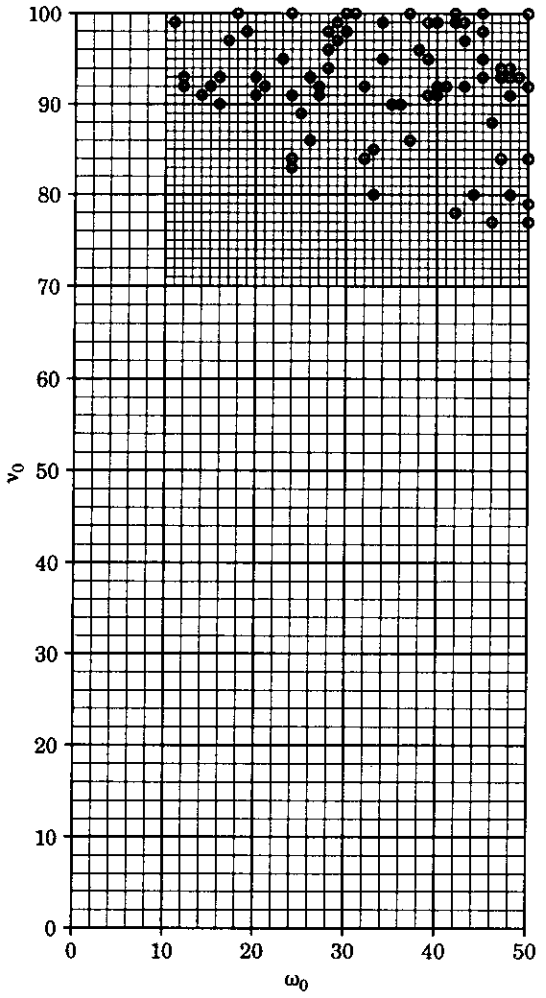

Figure 8. Eight-term approximation stable and unstable points in the v_0–ω_0 plane (all intersection points without a label indicate stable points, whereas circled ones indicate unstable points).

Comparing equation (26) with equation (27), one may define the parameter ϵ as

$$\epsilon = v_0/L, \tag{28}$$

and the matrices in equation (27) are defined as

$$\mathbf{C}(t) = \begin{bmatrix} 0 & -\frac{16}{3} \\ \frac{16}{3} & 0 \end{bmatrix} \sin \omega_0 t, \tag{29}$$

$$\mathbf{B}(0) = \begin{bmatrix} \left(\dfrac{2P_0}{\rho A} - \kappa v_0^2\right)\dfrac{\pi^2}{2L^2} & 0 \\ 0 & \left(\dfrac{2P_0}{\rho A} - \kappa v_0^2\right)\dfrac{2\pi^2}{L^2} \end{bmatrix}, \tag{30}$$

$$\mathbf{B}(t) = \begin{bmatrix} 0 & -8\omega_0/3 \\ 8\omega_0/3 & 0 \end{bmatrix} \cos \omega_0 t + \begin{bmatrix} \kappa v_0 \pi^2/2L & 0 \\ 0 & 2\kappa v_0 \pi^2/L \end{bmatrix} \cos 2\omega_0 t. \tag{31}$$

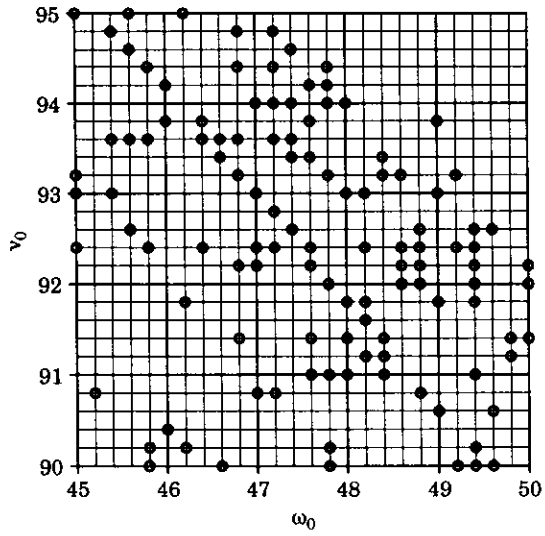

Figure 9. Eight-term approximation stable and unstable points for a small region in the v_0–ω_0 plane (all intersection points without a label indicate stable points, whereas circled ones indicate unstable points).

It is of interest to note that $\mathbf{B}(t)$ in equation (31) involves both $\cos \omega_0 t$ and $\cos 2\omega_0 t$ terms; the latter approaching zero as κ approaches zero. Thus, in the two-term approximation for non-zero κ, parametric excitation occurs at both the velocity variation frequency ω_0 and at twice that frequency. It is only the double frequency $2\omega_0$ which appears in equations (23) or (24) associated with the one-term approximation. Note also that the part of $\mathbf{B}(t)$ associated with the double frequency is of order ϵ and thus very small for small ϵ.

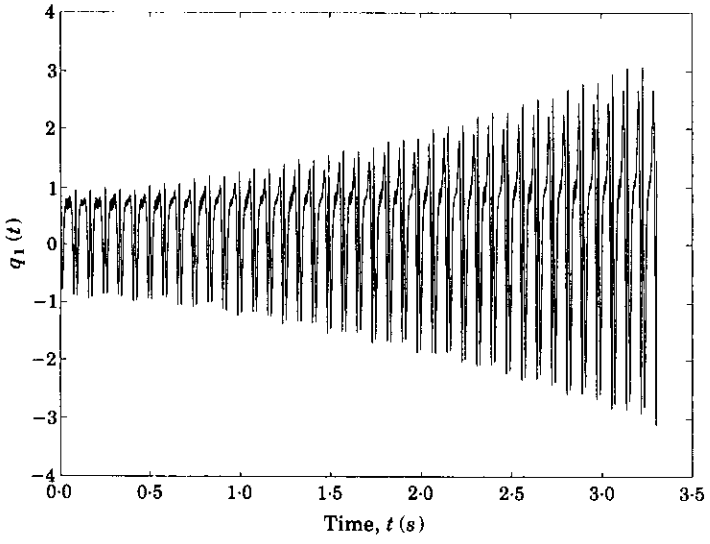

Figure 10. The first generalized displacement *vs.* time for $v_0 = 92$, $\omega_0 = 38$, using the two-term approximation.

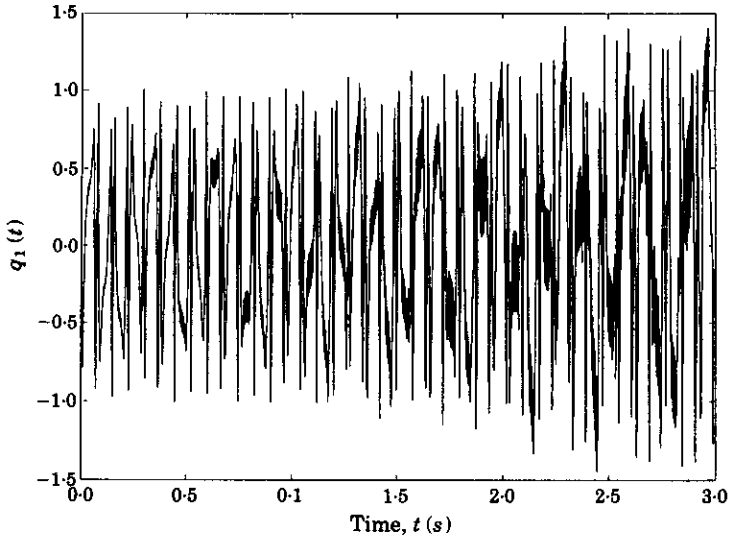

Figure 11. The first generalized displacement *vs.* time for $v_0 = 90$, $\omega_0 = 42$, using the four-term approximation.

In reference [12], it is stated that for small ϵ instability *may* occur at critical excitation frequencies ω_0 in the neighbourhood of

$$(\Omega_i + \Omega_j)/s \quad \text{and} \quad (\Omega_i - \Omega_j)/s, \qquad i, j, s = 1, 2, \ldots, n, \tag{32}$$

where the specific Ω_i's, which are the diagonal terms of $\mathbf{B}(0)$, are defined as

$$\Omega_i = \left(\frac{2P_0}{\rho A} - \kappa v_0^2\right)\frac{i^2\pi^2}{2L^2}. \tag{33}$$

Note that although equations (29)–(31) for the two-term approximation were given as an example, equations (32) and (33) are valid for any n-term approximation of the system. Only the two- and four-term approximations are considered, and the critical excitation

TABLE 2

The Floquet multipliers for the two-term approximation for unstable points

v_0	w_0	Magnitude of eigenvalues			
58	50	1·000000	1·000000	0·998776	1·001226
75	50	1·000000	1·000000	0·974578	1·026085
79	48	0·990363	0·990363	1·009731	1·009731
82	45	1·000000	1·000000	0·983430	1·016849
84	22	1·000000	1·000000	0·981328	1·019027
84	35	1·000000	1·000000	0·969742	1·031202
89	40	1·000000	1·000000	0·937217	1·066989
91	31	1·000000	1·000000	0·945522	1·057616
92	38	1·000000	1·000000	0·954281	1·047909
92	50	1·000000	1·000000	0·935442	1·069013
93	25	1·000000	1·000000	0·955228	1·046871
94	48	1·000000	1·000000	0·936450	1·067863
96	35	1·000000	1·000000	0·964450	1·036860
99	33	1·000000	1·000000	0·963471	1·037913

TABLE 3

The Floquet multipliers for the four term approximation for unstable points

v_0	w_0	Magnitude of eigenvalues							
83	42	1·000000	1·000000	1·000000	1·000000	1·000000	1·000000	0·973545	1·027174
85	30	1·016025	1·016025	0·984228	1·984228	1·000000	1·000000	1·000000	1·000000
85	39	1·000000	1·000000	0·972413	0·972413	1·028370	1·028370	1·000000	1·000000
85	47	1·000000	1·000000	1·000000	1·000000	1·000000	1·000000	0·995872	1·004145
86	27	1·000000	1·000000	1·000000	1·000000	1·000000	1·000000	0·978738	1·021724
86	40	1·000000	1·000000	1·000000	1·000000	1·000000	1·000000	0·965511	1·035721
87	26	1·000000	1·000000	1·000000	1·000000	0·992755	0·992755	1·007298	1·007298
87	29	1·024330	1·024330	0·976248	0·976248	1·000000	1·000000	1·000000	1·000000
87	47	1·000000	1·000000	1·000000	1·000000	1·000000	1·000000	0·948808	1·053954
89	28	1·012385	1·012385	0·987766	0·987766	1·000000	1·000000	1·000000	1·000000
89	38	1·000000	1·000000	1·000000	1·000000	1·000000	1·000000	0·966621	1·034532
90	19	1·000000	1·000000	1·000000	1·000000	1·000000	1·000000	0·972739	1·028025
90	42	1·024769	1·024769	1·000000	1·000000	0·975830	0·975830	1·000000	1·000000
91	14	1·000000	1·000000	1·019057	1·019057	0·981299	0·981299	1·000000	1·000000
91	44	1·000000	1·000000	1·000000	1·000000	1·000000	1·000000	0·934576	1·070003
91	48	1·000000	1·000000	1·000000	1·000000	1·000000	1·000000	0·970156	1·030762
92	30	1·000000	1·000000	1·000000	1·000000	0·964849	0·964849	1·036431	1·036431
92	38	1·000000	1·000000	1·000000	1·000000	1·000000	1·000000	0·942544	1·060959
92	43	1·000000	1·000000	0·986306	0·986306	1·013884	1·013884	1·000000	1·000000
92	50	1·000000	1·000000	0·943917	0·943917	1·059415	1·059415	1·000000	1·000000
93	18	1·000000	1·000000	1·000000	1·000000	1·000000	1·000000	0·976308	1·024267
93	47	1·000000	1·000000	1·009187	1·009187	0·990897	0·990897	1·000000	1·000000
93	49	1·000000	1·000000	1·000000	1·000000	1·000000	1·000000	0·897785	1·113852
93	50	1·000000	1·000000	1·000000	1·000000	0·967623	0·967623	1·033460	1·033460
94	28	1·000000	1·000000	1·000000	1·000000	1·000000	1·000000	0·983419	1·016861
95	24	1·000000	1·000000	1·000000	1·000000	1·000000	1·000000	0·977245	1·023285
96	27	1·000000	1·000000	1·000000	1·000000	1·000000	1·000000	0·979253	1·021187
96	40	1·000000	1·000000	1·000000	1·000000	1·000000	1·000000	0·967680	1·033399
96	46	1·000000	1·000000	1·000000	1·000000	1·000000	1·000000	0·946831	1·056155
97	43	1·000000	1·000000	1·000000	1·000000	1·000000	1·000000	0·969917	1·031016
100	13	1·000000	1·000000	1·000000	1·000000	1·000000	1·000000	0·924064	1·082176

frequencies are calculated from equations (32) and (33). For small values of ϵ, the value of v_0 is very small. Our previous Floquet results indicate that no instabilities can be expected for small v_0 values, except possibly for unrealistically large ω_0 values. Taking $v_0 = 0{\cdot}01$, so that $\epsilon = 0{\cdot}0272$ is also small, and using the two- and four-term approximations, leads to the results summarized in Tables 4 and 5. These tables, for the value of

TABLE 4

The Floquet multipliers for the points at which instability may occur [12] *(two-term approximation)*

v_0	w_0	Magnitude of eigenvalues			
0·01	185·5	1·000000	1·000000	1·000000	1·000000
0·01	371·0	1·000000	1·000000	1·000000	1·000000
0·01	556·5	1·000000	1·000000	1·000000	1·000000
0·01	742·0	1·000000	1·000000	1·000000	1·000000
0·01	1113·0	1·000068	1·000068	0·999932	0·999932
0·01	1484·0	1·000000	1·000000	1·000000	1·000000

TABLE 5

The Floquet multipliers for the points at which instability may occur [12] (*four-term approximation*)

v_0	w_0	Magnitude of eigenvalues							
0·01	92·8	1·000000	1·000000	1·000000	1·000000	1·000000	1·000000	1·000000	1·000000
0·01	123·7	1·000000	1·000000	1·000000	1·000000	1·000000	1·000000	1·000000	1·000000
0·01	185·5	1·000000	1·000000	1·000000	1·000000	1·000000	1·000000	1·000000	1·000000
0·01	247·0	1·000000	1·000000	1·000000	1·000000	1·000000	1·000000	1·000000	1·000000
0·01	278·0	1·000000	1·000000	1·000000	1·000000	1·000000	1·000000	1·000000	1·000000
0·01	371·0	1·000000	1·000000	1·000000	1·000000	1·000000	1·000000	1·000000	1·000000
0·01	464·0	1·000000	1·000000	1·000000	1·000000	1·000000	1·000000	1·000000	1·000000
0·01	495·0	1·000000	1·000000	1·000000	1·000000	1·000000	1·000000	1·000000	1·000000
0·01	556·5	1·000000	1·000000	1·000000	1·000000	1·000000	1·000000	1·000000	1·000000
0·01	618·0	1·000000	1·000000	1·000000	1·000000	1·000000	1·000000	1·000000	1·000000
0·01	649·0	1·000000	1·000000	1·000000	1·000000	1·000000	1·000000	1·000000	1·000000
0·01	742·0	1·000000	1·000000	1·000000	1·000000	1·000000	1·000000	1·000000	1·000000
0·01	866·0	1·000000	1·000000	1·000000	1·000000	1·000000	1·000000	1·000000	1·000000
0·01	927·5	1·000000	1·000000	1·000000	1·000000	1·000000	1·000000	1·000000	1·000000
0·01	989·0	1·000000	1·000000	1·000000	1·000000	1·000000	1·000000	1·000000	1·000000
0·01	1113·0	1·000055	1·000055	0·999945	0·999945	1·000000	1·000000	1·000000	1·000000
0·01	1298·0	1·000000	1·000000	1·000000	1·000000	1·000000	1·000000	1·000000	1·000000
0·01	1484·0	1·000000	1·000000	1·000000	1·000000	1·000000	1·000000	1·000000	1·000000
0·01	1855·0	1·000038	1·000038	0·999962	0·999962	0·999973	0·999973	1·000027	1·000027
0·01	2226·0	1·000000	1·000000	1·000000	1·000000	1·000000	1·000000	1·000000	1·000000
0·01	2597·0	1·000021	1·000021	0·999979	0·999979	1·000000	1·000000	1·000000	1·000000
0·01	2968·0	1·000000	1·000000	1·000000	1·000000	1·000000	1·000000	1·000000	1·000000

$v_0 = 0{\cdot}01$, show the ω_0 values at *potential* instabilities as identified by equations (32) and (33). Also shown in the tables are the Floquet multipliers obtained by numerical solution of the two-term (Table 4) and four-term (Table 5) approximations. It is shown in Table 4 that only one of the potential instability points is actually unstable for the two-term approximation, and that this occurs at a large value of $\omega_0 = 1113$. Similarly, it is shown in Table 5 that only three of the potential instability points are actually unstable; for values of $\omega_0 = 1113$, 1855 and 2597. Note that the excitation frequencies ω_0, at which instabilities occur for $v_0 = 0{\cdot}01$, are very large and lie well outside the v_0–ω_0 regions shown in Figures 5–8. Also, note that equations (32) and (33) predict an increase in the number of potential instability points with an increase in the number of terms (n) in the approximate solution. This trend is in agreement with the increase in the number of actual unstable points with n as in both Tables 4 and 5 and Figures 5–8.

5. SUMMARY AND CONCLUSIONS

The transverse vibration of an axially accelerating string has been investigated. First, the equation of motion is derived for small transverse displacements and large axial tension values. The partial differential equation governing the motion is discretized using Galerkin's method. Taking one term in the Galerkin approximation yields the Mathieu equation. Taking two terms leads to gyroscopically coupled ordinary differential equations. The first- and second-term equations are fundamentally different systems, and the first-term solutions are used only to check the Floquet solutions against the well-known analytical solutions. The one-term and three-term approximation solutions look qualitatively similar to each other. Because of the gyroscopic coupling, the even-term approximations represent the system behaviour better, and

extensive numerical calculations for two-, four-, six- and eight-term approximations were performed.

A major conclusion from the calculations is that $v_0 > 70$ and $\omega_0 > 10$ is a critical region with a high likelihood of instability. These velocities and excitation frequencies are much higher than those that might be encountered in real engineering devices. Increasing the number of terms leads to better results through convergence, and the unstable points cluster more. However, the equations are highly sensitive to v_0 and ω_0 values and, as a consequence, a small area in the v_0–ω_0 plane is mapped to a very large area in the δ–ϵ plane. The reason why results are displayed in the v_0–ω_0 plane is to facilitate interpretation in terms of the velocity amplitude and frequency. The Floquet solutions are also compared with the analytical solutions given in reference [12] for small ϵ perturbation parameters. From the analytical solution, it is evident that for higher approximations one is more likely to obtain unstable points at lower excitation frequencies. This was also observed in the numerical calculations. The analytical solutions and the Floquet solutions are in reasonable agreement. Simulations for some unstable points confirm the stability results. The simulation approach shows that the instabilities are weaker for the higher order approximations.

This initial investigation of the transverse vibration of an axially accelerating string has indicated some areas for further research. Topics for further investigation in axially accelerating systems include experimental validation, consideration of transport velocity functions other than a sinusoid, and sensitivity studies for parameters such as P_0 and κ. Also, in the Galerkin's approximation stationary string eigenfunctions were used, and these could be replaced by the moving string eigenfunctions given in reference [10] for improved convergence in systems with velocity variations about a constant nominal axial speed.

ACKNOWLEDGMENTS

The authors would like to thank Professor A. H. Nayfeh for providing research facilities to M.P., and Dr Marwan Bikdash for his helpful suggestions, also to M.P.

REFERENCES

1. R. SKUTCH 1987 *Annalen der Physik und Chemie* **61**, 190–195. Uber die Bewegung eines gespannten Fadens welcher gezwungen ist, durch zwei feste Punkte mit einer konstanten Geschwindigkeit zu gehen und zwischen denselben in Transversalschwingungen von geringer Amplitude versetzt wird.
2. R. A. SACK 1952 *British Journal of Applied Physics* **5**, 224–226. Transverse oscillations in travelling strings.
3. A. G. ULSOY, C. D. MOTE, JR. and R. SZYMANI 1978 *Holz als Roh und Werkstoff* **36**, 273–280. Principal developments in band saw vibration and stability research.
4. J. A. WICKERT and C. D. MOTE, JR. 1988 *Shock and Vibration Digest* **20**(5), 3–13. Current research on the vibration and stability of axially moving materials.
5. A. G. ULSOY and C. D. MOTE, JR. 1982 *American Society of Mechanical Engineers Journal of Engineering for Industry* **104**, 1–8. Vibration of wide bandsaw blades.
6. A. G. ULSOY, J. E. WHITESELL and M. D. HOOVEN 1985 *American Society of Mechanical Engineers, Journal of Vibration, Acoustics, Stress and Reliability in Design* **107**, 282–290. Design of belt tensioner systems for dynamic stability.
7. S. CHONAN 1986 *Journal of Sound and Vibration* **107**, 155–165. Steady state response of an axially moving strip subjected to a stationary lateral load.
8. J. A. WICKERT and C. D. MOTE, JR. 1989 *Journal of the Acoustical Society of America* **85**, 1365–1368. On the energetics of axially moving continua.

9. J. A. WICKERT and C. D. MOTE, JR. 1988 *Journal of the Acoustical Society of America* **84**, 963–969. Linear transverse vibration of an axially moving string-particle system.
10. J. A. WICKERT and C. D. MOTE, JR. 1990 *American Society of Mechanical Engineers, Journal of Applied Mechanics* **57**, 738–744. Classical vibration analysis of axially moving continua.
11. W. L. MIRANKER 1960 *IBM Journal of Research and Development* **4**(1), 36–42. The wave equation in a medium in motion.
12. C. S. HSU 1963 *American Society of Mechanical Engineers, Journal of Applied Mechanics* **30**, 367–372. On the parametric excitation of a dynamic system having multiple degrees of freedom.
13. H. MCCALLION 1973 *Vibration of Linear Mechanical Systems*. New York: John Wiley.
14. L. MEIROVITCH 1980 *Computational Methods in Structural Dynamics*. Groningen, The Netherlands: Sijthoff and Noordhoff.
15. H. JEFFREYS and B. SWIRLES 1956 *Methods of Mathematical Physics*. Cambridge: Cambridge University Press.
16. C. D. MOTE, JR. 1965 *Journal of the Franklin Institute* **279**(6), 431–444. A study of bandsaw vibrations.
17. L. MEIROVITCH 1970 *Methods of Analytical Dynamics*. New York: McGraw-Hill.
18. A. H. NAYFEH and D. T. MOOK 1979 *Nonlinear Oscillations*. New York: John Wiley.
19. A. STOFFEL 1990 *Zeitschrift für angewandte Mathematik und Mechanik* **70**, 1963–1972. Application of block analysis to the stability investigation of investigation of Hamiltonian systems of linear differential equations with periodic coefficients.
20. V. A. YAKUBOVITCH and V. M. STARZHINSKII 1975 *Linear Differential Equations with Periodic Coefficients*. New York: John Wiley.
21. D. A. STREIT, C. M. KROUSGRILL and A. K. BAJAJ 1986 *Journal of Dynamic Systems, Measurement and Control* **108**, 206–214. A preliminary investigation of the dynamic stability of flexible manipulators performing repetitive tasks.
22. F. R. ARCHIBALD and A. G. EMSLIE 1956 *American Society of Mechanical Engineers, Journal of Applied Mechanics* **25**, 347–348. Vibration of a string having a uniform motion along its length.

APPENDIX: LIST OF SYMBOLS

T	kinetic energy	w_j	weighting functions
V	potential energy	$\mathbf{M}, \mathbf{C}, \mathbf{K}$	coefficients matrices in equation (13)
t	time		
δ	variation	v_0	axial velocity amplitude
ρ	density	ω_0	frequency of axial velocity variation
A	cross-sectional area		
y	transverse displacement	P_0	initial tension
x	spatial variable	η	a constant $(0 \leqslant \eta \leqslant 1)$
v	axial velocity	κ	pulley support parameter
L	length	δ	a parameter in Mathieu equation
P	tension		
e	strain	ε	a parameter in Mathieu equation
E	Young's modulus		
F	force	ϵ	perturbation parameter
Δ	total longitudinal displacement	$\mathbf{X}$	solution vector in equation (27)
$q_i(t)$	generalized displacements	$\mathbf{C}(t), \mathbf{B}(0), \mathbf{B}(t)$	coefficient matrices in equation (27)
$\mathbf{q}$	generalized displacement vector	Ω_i	frequencies which are diagonal terms of $\mathbf{B}(0)$
R	residual		